

Jay X. Tang · Josef A. Käs · Jagesh V. Shah
Paul A. Janmey

Counterion-induced actin ring formation

Received: 24 May 2001 / Revised version: 19 July 2001 / Accepted: 19 July 2001 / Published online: 8 September 2001
© EBSA 2001

Abstract Actin filaments form rings and loops when >20 mM divalent cations are added to very dilute solutions of phalloidin-stabilized filamentous actin (F-actin). Some rings consist of very long single actin filaments partially overlapping at their ends, and others are formed by small numbers of filaments associated laterally. In some cases, undulations of the rings are observed with amplitudes and dynamics similar to those of the thermal motions of single actin filaments. Lariat-shaped aggregates also co-exist with rings and rodlike bundles. These polyvalent cation-induced actin rings are analogous to the toroids of DNA formed by addition of polyvalent cations, but the much larger diameter of actin rings reflects the greater bending stiffness of F-actin. Actin rings can also be formed by addition of streptavidin to crosslink sparsely biotinylated F-actin at very low concentrations. The energy of bending in a ring, calculated from the persistence length of F-actin and the ring diameter, provides an estimate for the adhesion energy mediated by the multivalent counterions, or due

to the streptavidin-biotin bonds, required to keep the ring closed.

Keywords Biopolymer · Polyelectrolyte · Attractive interaction · Cytoskeletal filaments · Cell motility

Introduction

The self-association of like-charged polymers caused by multivalent counterions is a commonly observed phenomenon for which a theoretical explanation is still an ongoing effort. In cases where a specific chemical bond between filaments, or a chemical crosslink due to the counterion, can be ruled out, a number of models based on spatial arrangement or fluctuations of counterions on the linear polyelectrolyte have been proposed to account for the attractive force. Most experimental tests of such models are derived from studies of double stranded DNA, and the general application of these models to other systems is limited. Some recent studies have emphasized that the polyelectrolyte properties of cytoskeletal polymers are similar to those of DNA, and predictions made from studies of DNA can be tested in these systems. A particularly striking form of counterion-mediated condensed DNA is toroids of single or multiple DNA molecules (Baeza et al. 1987). The condensed DNA toroids are preferentially formed when the DNA is too dilute to form large lateral aggregates, and the average diameter of the toroids is comparable to the persistence length of DNA. The same concepts applied to other charged filaments suggest that they too may form similar rings whose structures may differ from those of DNA toroids in a manner predictable by differences in linear charge density, filament diameter, bending stiffness, etc.

Actin is a highly expressed cytoskeletal protein that plays essential roles in the mechanical properties of eukaryotic cells, as well as with their division and locomotion properties (Condeelis 1993; Stossel 1993). Control of these functions depends on remodeling of

J.X. Tang (✉)
Department of Physics,
Indiana University, Swain West 165,
727 East Third Street, Bloomington, IN 47405, USA
E-mail: jxtang@indiana.edu
Fax: +1-812-8555533

J.A. Käs
Center for Nonlinear Dynamics,
Physics Department & Institute for Cellular and Molecular
Biology & Center for Nano and Molecular Science,
University of Texas at Austin, Austin, TX 78712, USA

J.V. Shah
Ludwig Institute for Cancer Research,
University of California, San Diego,
9500 Gilman Drive, La Jolla, CA 92093, USA

P.A. Janmey
Departments of Physiology and Physics & Astronomy,
Institute for Medicine and Engineering,
University of Pennsylvania, Vagelos Labs,
3340 Smith Walk, Philadelphia, PA 19104, USA

networks composed of the filamentous actin (F-actin), which undergoes dynamic assembly and disassembly, as well as crosslinking and lateral association both *in vitro* and *in vivo* (Alberts et al. 1994; Carlier et al. 1994; Kawamura and Maruyama 1970; Oosawa 1993). F-actin is a linear protein filament with a diameter of 8 nm, a persistence length approximately 17 μm (Gittes et al. 1993; Isambert et al. 1995; Ott et al. 1993), and a nominal charge density of 11 negative fundamental charges per monomer subunit, or $-4e^-$ per nm along the filament axis (Tang and Janmey 1996). Previous studies have established the polyelectrolyte nature of F-actin, and consequently the lateral association of F-actin to form large bundles induced by polyvalent counterions (Tang and Janmey 1996; Tang et al. 1997; Xian et al. 1999). This report documents the formation of actin rings and lariat-shaped aggregates induced by a simple divalent metal ion, Mg^{2+} . Microscopic observations of size, shape, and undulations of the actin rings are related to the measured stiffness of F-actin. Actin rings are also formed using streptavidin to crosslink sparsely biotinylated F-actin, allowing a comparison between the lateral adhesive force due to electrostatic attraction and that due to a specific type of biochemical crosslink.

Materials and methods

Actin was purified according to the method described by Spudich and Watt (1971). The monomeric globular (G)-actin was kept in a nonpolymerizing buffer containing 4 mM Hepes at pH 7.5, 0.2 mM CaCl_2 , 0.5 mM adenosine triphosphate (ATP), 0.2 mM dithiothreitol (DTT), and 0.5 mM sodium azide (NaN_3). F-actin was polymerized from G-actin by 150 mM KCl. Biotinylated actin was purchased from Cytoskeleton (Denver, Co., USA). Streptavidin was purchased from Molecular Probes (Eugene, Ore., USA). All chemicals were of analytical grade, supplied by either Sigma (St. Louis, Mo., USA) or ICN Pharmaceuticals (Costa Mesa, Calif., USA).

For microscopic observation, TRITC-labeled phalloidin was added to the polymerized actin at a 1:1 molar ratio. Then a small aliquot of the stock F-actin solution was diluted to nanomolar concentrations, followed by adding MgCl_2 to 50 mM. Alternatively, biotinylated G-actin was mixed with unlabeled G-actin at a 1:4 molar ratio, and the mixture was polymerized as above with TRITC-labeled phalloidin. Upon dilution to nanomolar protein concentration so that the solution contained only about one F-actin per $(10 \mu\text{m})^3$ volume, streptavidin, a tetrafunctional ligand for biotin, was added at a ratio of 1 avidin per 2 biotins in order to crosslink F-actin, with the expectation that intra-filament links would trap looped structures or rings.

Fluorescently labeled F-actin was visualized on a Nikon Diaphot 300 inverted microscope equipped with epifluorescence optics and a Nikon PlanApo 60 \times (NA 1.40) or PlanFluor 100 \times (NA 1.30) objective. The motions of the filaments were captured to a DAGE-MTI silicon intensified target (SIT) camera (DAGE-MIT, Michigan, IL) through a 2 \times optical coupler, and digitized to a Macintosh computer (Apple Computer, Cupertino, Calif.) through a Scion AG-5 video capture board (Scion Corporation, Frederick, MD). The images were typically captured at 15 frames/s for up to 1000 frames. Motions of the labeled filaments were simultaneously recorded to VHS videotape, which allowed alternative image capturing and additional analysis. Filaments that diffused out of the focal plane were not used in the analysis.

For each digitized frame, the fluorescent filament image was traced using an automated algorithm as described below, and the

coordinates saved to a file. The algorithm design was based on the point spread function of the microscope.

The intensity profile of a fluorescent filament is well approximated by a Gaussian function. The filament tracing algorithm begins by slicing through the local intensity profile and finds the best fit to a quadratic function. A quadratic function is used to compute the local intensity profile because its computation is simpler and faster than a Gaussian fit and it approximates the local profile near the intensity maximum. The quadratic function is computed over a number of orientations with respect to the filament. The steepest quadratic with an acceptable correlation coefficient is chosen to be the local intensity profile of the filament. In this way the algorithm determines both the actual orientation of the filament and the local intensity maximum, i.e. the approximate location of the filament in space. The algorithm proceeds by advancing along the calculated orientation of the filament and recalculating the local quadratic functions. Through this iterative scheme the filament contour can be determined. When the algorithm reaches a region that overlaps the starting point, the tracing of the ring is complete.

Analyzing real fluorescent filaments can be difficult owing to the presence of noise, both electronic and fluorescent. Before being traced, each video frame undergoes a pre-processing step using a log-Gaussian filter with spatial frequency optimized for the width of the fluorescent filament signal to enhance the filament intensity with respect to the background noise. Ring filament contour coordinates are analyzed to determine center of mass, which is then set as the origin of azimuthal coordinates.

Results

Formation of actin rings and other structures

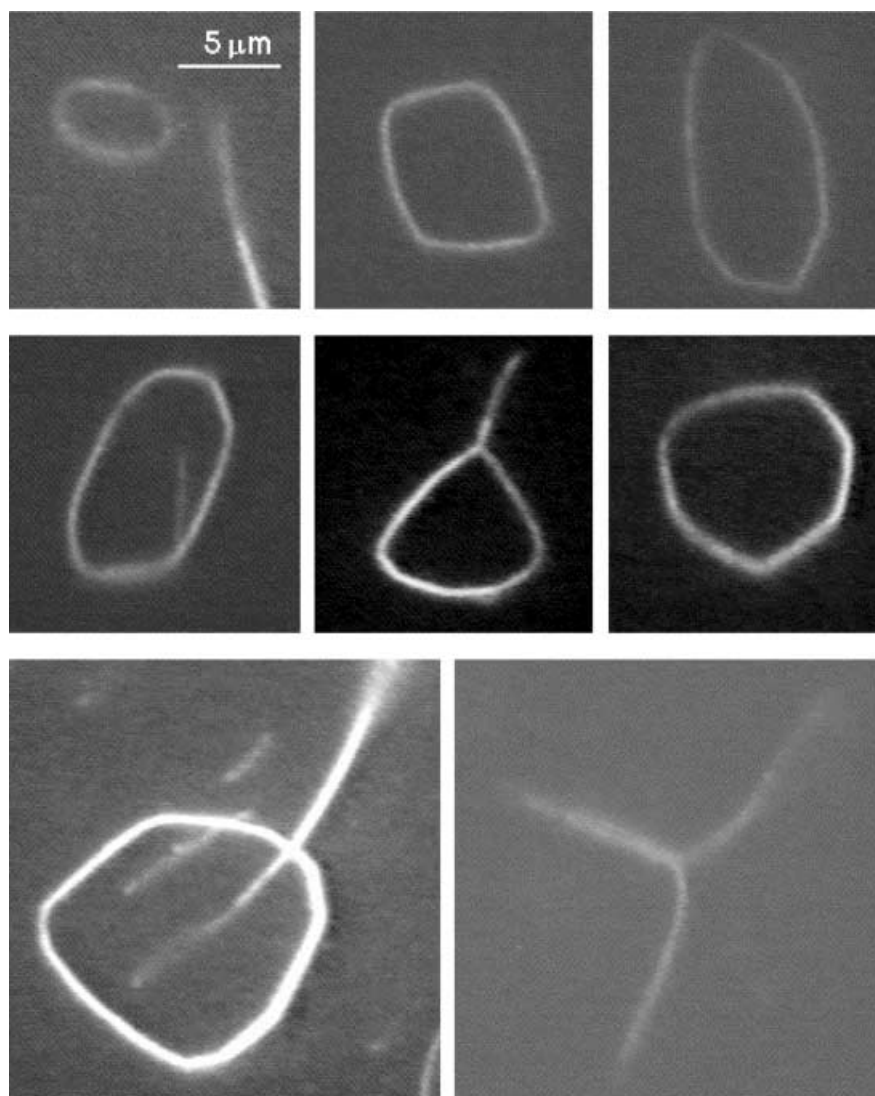
Actin filaments exhibit self-attractive interactions after addition of sufficient divalent metal ions, such as 50 mM MgCl_2 , as used in this study. When MgCl_2 was added into a very dilute F-actin solution in the nanomolar range, we occasionally observed that a subset of actin filaments assembled into various structures distinct from rodlike bundles, such as branched lateral aggregates and loops with or without additional tail(s) (Fig. 1). In rare cases, the two ends of a single filament adhered to each other to form an actin ring with fluorescence intensity through much of its contour comparable to that of a single labeled filament. The upper left image of Fig. 1 shows an example of an actin ring formed by a single long filament of 15–20 μm contour length.

Actin rings formed by a number of filaments are often kinked, and the kinks appear to be where some filaments end, discernible by a marked difference in fluorescence intensity over a particular kink. Also, segments with relatively higher fluorescence intensities appear to bear less bending, another indication of more filaments packed in the bundle.

Undulation of actin rings in solution

Although most of the images shown in Fig. 1 represent structures bound to the surface of glass slides, various looped structures were also observed in solution. The closed rings adherent to the glass substrate were likely formed in solution, although the strong anchoring effect

Fig. 1 Representative images of actin loops and other conformations of actin bundles. All structures were formed by adding MgCl_2 to 50 mM to a dilute suspension (5 nM) of F-actin. Actin filaments were stabilized by equimolar TRITC-phalloidin. *Scale bar* applies to all images



to the glass surface helped stabilize the otherwise dynamic and relatively weak interactions holding the closed structures. Occasionally, free-standing actin rings were observed, some of which either drifted off the microscope focal plane, or unraveled after some random observation times. Figure 2 shows a sequence of images of an actin ring undulating in solution. Traces of the filament at various times revealed the motions of the ring. There are two fixed positions, possibly representing points of adherence to the glass substrate. Traces from the images shown in Fig. 2a–h are superimposed in Fig. 2i. The possible anchorage positions can be noted, as well as an arc segment of large undulations between $\theta = -20$ and $+70^\circ$.

Figure 3 plots the traced positions of ring edge along three representative orientations, as marked in Fig. 2i. The origin of the coordinate is the center of mass of the ring, determined separately for each traced ring image. The lowest mode of undulations had a time constant on the order of 1 s. Owing to significant undulations of the

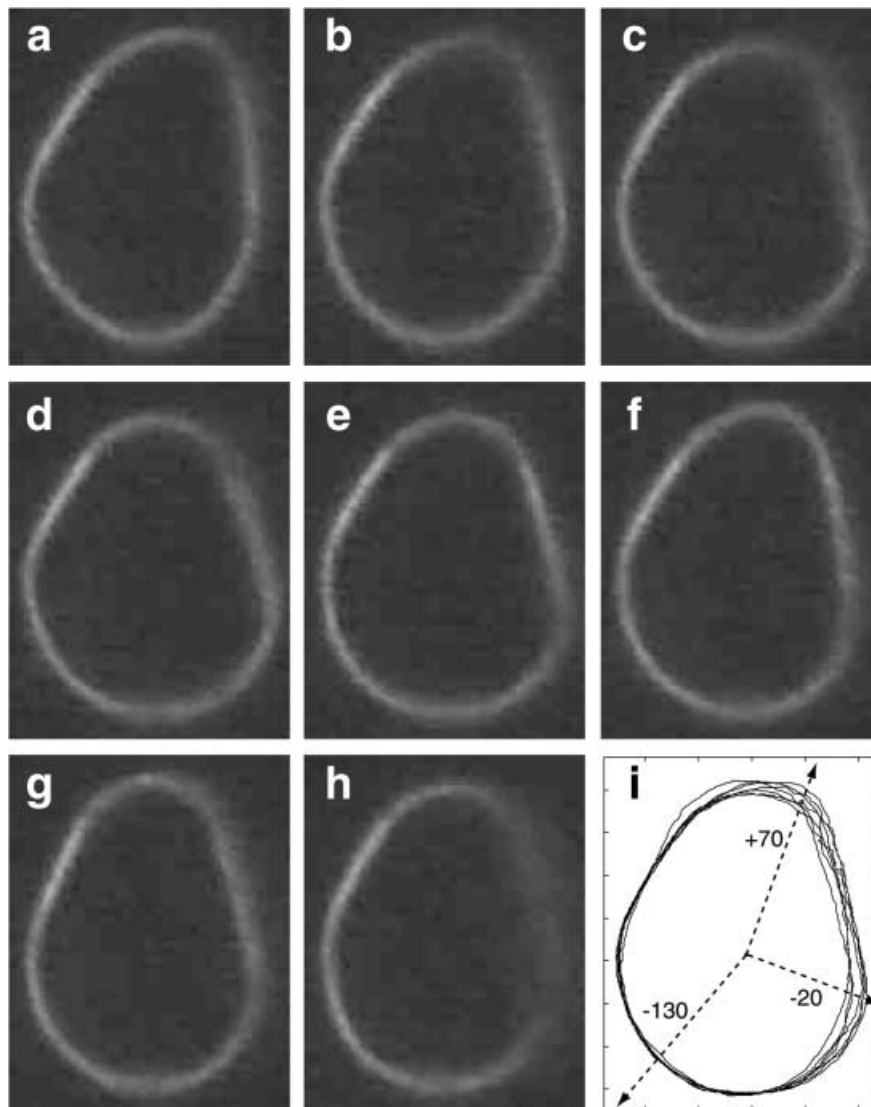
ring contour in and out of the focal plane, even with two points fixed, a continuous sequence of traceable images only covered a duration of 3 s or so, taken at the rate of 15 frames per second. The traced position data did not show clear periodic repeats over such a short duration.

Estimate of the adhesion energy causing the ring formation

If one assumes that the interaction between two filament ends is dynamic enough to allow adjustment in overlap when an actin ring is formed, the electrostatic adhesion energy between the filament ends can be estimated by measuring the diameter and overlap of an actin ring (see Appendix). The adhesion energy per unit length can be equated to the bending energy of the ring, calculated as:

$$v = \frac{\kappa L}{\pi R^3} = \frac{2kTL_p L}{\pi R^3} \quad (1)$$

Fig. 2 Representative images of an undulating actin ring (**a–h**). The traces of the eight conformations are overlaid in (**i**) to show regions of undulations, as well as points of adhesion to the glass substrate. The image magnification is the same as in Fig. 1



(see Eq. 5 in the Appendix), where L_p is the persistence length, L is the contour length, and R is the radius of the ring. Based on the images shown in Fig. 2, if one takes $17\ \mu\text{m}$ as the persistence length of F-actin (Isambert et al. 1995), $6.7\ \mu\text{m}$ as the average diameter of this particular ring, $26\ \mu\text{m}$ as its contour length, and the overlap of about one quarter of the ring contour, the adhesion energy due to the counterion-mediated attractive force is estimated to be on the order of $7.5\ \text{kT}/\mu\text{m}$, or $3.1 \times 10^{-9}\ \text{erg}/\text{cm}$ at $25\ ^\circ\text{C}$.

Actin rings formed by streptavidin-crosslinked biotinylated actin filaments

The formation of actin rings is novel, but the mechanism of counterion-mediated end-to-end interaction is not uniquely required. We found that actin rings also form when dilute solutions of F-actin covalently labeled by biotin were mixed with streptavidin, a tetrafunctional

ligand for biotin. Since streptavidin has no direct effect on actin structure, ring closure would only take place when thermal motions or local shear flow brought two ends of a filament in close enough proximity for streptavidin to capture biotin moieties at both ends. Figure 4 shows nine randomly recorded actin rings. The rings formed by streptavidin-crosslinked biotinylated F-actin were significantly smaller than those formed by $50\ \text{mM}\ \text{MgCl}_2$, suggesting a stronger adhesion energy (see Appendix). The average ring diameter is $2.4\ \mu\text{m}$, with a standard deviation of $0.4\ \mu\text{m}$ for the nine rings shown in Fig. 4. Owing to the extremely strong binding between biotin and streptavidin [affinity $2.5 \times 10^{13}\ \text{M}^{-1}$ (Green 1990)], a small number of biotin-streptavidin bonds provide enough adhesion energy to stabilize these actin rings. The number of bonds can be estimated according to Eq. 8 in the Appendix, i.e.:

$$n = \frac{4\pi L_p}{R \ln(K_a)} = \frac{4 \times 3.14 \times 17\ \mu\text{m}}{1.2\ \mu\text{m} \times \ln(2.5 \times 10^{15})} = 5.0 \quad (2)$$

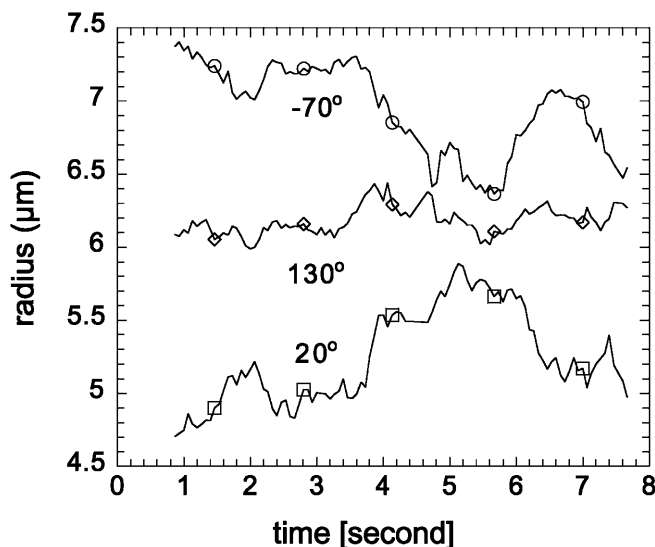
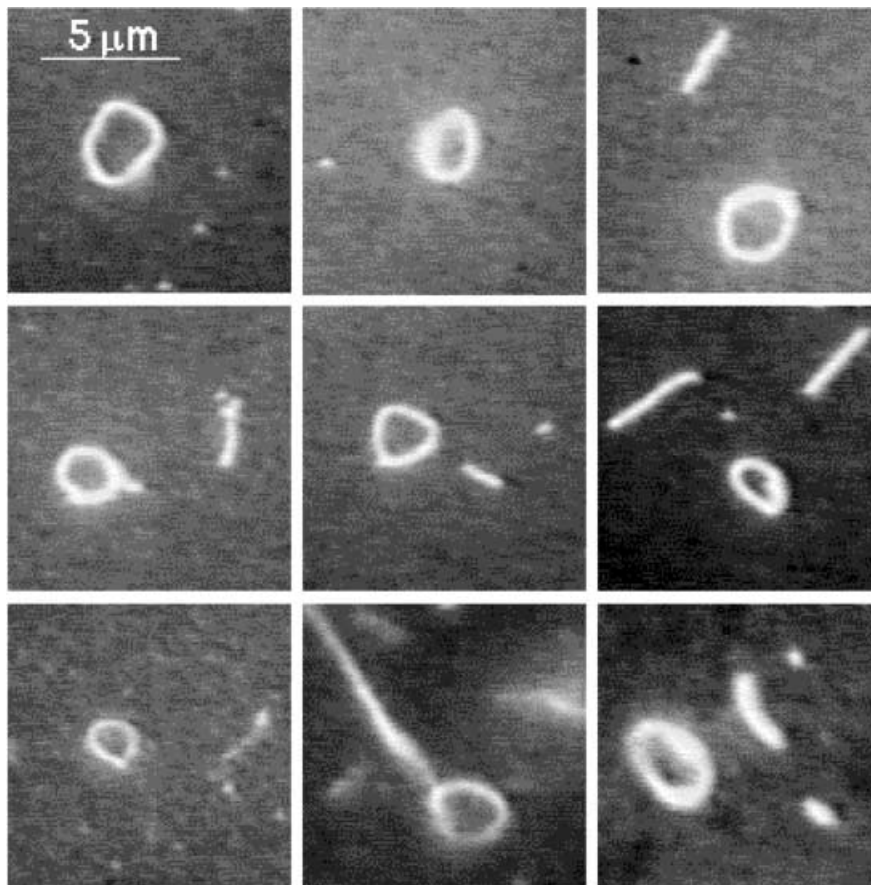


Fig. 3 Time course of three positions along the ring contour as shown in Fig. 2. The positions along all three orientations are plotted as their distances from the origin of coordinates, which is the calculated center of mass of the ring

Note that the number of bonds required for the ring formation is directly proportional to the persistence length of F-actin, taken as $17 \mu\text{m}$ for this estimate.

Fig. 4 A collection of nine actin rings formed by biotin-streptavidin crosslinking. Approximately 20% of actin protomers were biotinylated, and the streptavidin tetramers were added in equimolar proportions. The diameter of these nine rings is measured to average $2.4 \mu\text{m}$, with a standard error of $0.4 \mu\text{m}$



Discussion

Fluorescence labeling of F-actin has enabled imaging of single filaments in solution (Yanagida et al. 1984), and determination of their thermal motions and hydrodynamic properties by quantitative image analysis (Gittes et al. 1993; Isambert et al. 1995; Kas et al. 1996; Ott et al. 1993). This technique has also allowed us to observe the formation of actin rings, as well as a variety of other looped structures formed by F-actin. An actin ring can be formed by either a small number of filaments, or less often, a single long filament. Since actin filaments are stiff, characterized by a rather large persistence length on the order of $10 \mu\text{m}$, the diameter of an actin ring is on the order of micrometers, much larger than that of DNA toroids. The stiff nature of F-actin is also responsible for the appearance of kinks along the contour of a loop formed by a number of filaments. Some kinks occur where one or more filaments end, while other kinks may represent a structural defect within an actin filament. An alternative analysis of the origin of kinks in the multi-filament actin rings has also recently been reported (Golestanian and Liverpool 2000). Some images we observed also resemble certain dynamical intermediates in the collapse of semiflexible polymers, as predicted by a recent Brownian dynamics simulation study (Schnurr et al. 2000). For instance, the lariat-shaped aggregates of

F-actin are perhaps the counterparts of the DNA “tennis racquets”, referring to a series of metastable intermediates present prior to the eventual formation of DNA toroids.

The divalent cation Mg^{2+} at concentrations of 50 mM clearly induces an attractive interaction that leads to formation of actin bundles when the actin concentration is high. The same electrostatic force accounts for the formation of actin rings and other looped or bifurcated structures when the solution of F-actin is extremely dilute. The mechanism of such an attractive interaction has been predicted theoretically to explain the phenomenon of DNA condensation (Bloomfield 1991; Dewey 1990; Manning 1978; Marquet and Houssier 1991; Oosawa 1971; Ray and Manning 1994; Rousina and Bloomfield 1996). A few years ago, we reported an experimental survey, suggesting the relevance of polyelectrolyte theories to polyvalent cation induced bundle formation of F-actin (Tang and Janmey 1996), as well as other highly negatively charged biopolymers such as microtubules, tobacco mosaic virus (TMV), and the filamentous bacteriophage fd (Tang et al. 1996). These recent experimental findings support the standing theoretical effort to predict attractive interactions between filaments of like charge (Gronbech-Jensen et al. 1997; Ha and Liu 1997; Lyubartsev et al. 1998; Nguyen and Shklovskii 2000). Our observations of actin ring formation further confirm the polyelectrolyte nature of F-actin, and demonstrate a rich structural variance of actin assemblies, which may stimulate additional theoretical interest.

The persistence length of F-actin has been determined by mode analysis for long actin filaments undulating while confined within a thin layer of less than 5 μm thickness (Gittes et al. 1993; Isambert et al. 1995; Ott et al. 1993). Such treatment is in principle equally applicable to the analysis of undulations along the contour of actin rings. However, under our experimental condition with the presence of 50 mM divalent magnesium salt, F-actin tends to anchor to the glass substrate, rendering the confinement technique impractical. Owing to this practical limitation, we did not attempt to determine the persistence length of F-actin in 50 mM Mg^{2+} , but instead, we adopt its literature value at more standard solution conditions for further analyses in this report. Although a large increase in ionic strength is likely to affect the electrostatic contribution to the stiffness of a polymer in solution, the magnitude of the predicted contribution of such an effect is negligible compared to the extremely large intrinsic persistence length of F-actin (Odijk 1977). However, different methods to measure F-actin stiffness lead to different values, and we note that recent reports of persistence length for actin range from 3 to 17 μm , so that our estimates of adhesion energies are also subject to this range of variation.

Despite the variable size and shape of the looped structures of F-actin, semi-quantitative information was obtained using the mathematical analysis described in

the Appendix. Two estimates of interaction energies have been presented in the Results section. For the actin ring shown in Fig. 2, the adhesion energy at the segment of overlap is estimated to be 7.5 kT per micrometer of filament overlap, using Eq. 5 in the Appendix. This value translates to about 0.02 kT per actin protomer in the overlap region. Given the fact that each actin protomer in F-actin retains about 10 negative charges, this experimental estimate of interaction energy is much smaller than a recent theoretical prediction for the energy of DNA condensation, which is estimated to be 0.07 kT per nucleotide (Nguyen and Shklovskii 2000). We note, however, that our estimate only sets a lower bound of the interaction energy by assuming that the counterion mediated attractive interaction is so weak that it allows for adjustment of the segment overlap. Moreover, a simple comparison with DNA also ignores the much larger surface area of F-actin and hence the divalent counterions can only mediate an attractive force involving a small fraction of the charged residues on the filament surfaces in the areas of close contact. In contrast, the relatively weak and delocalized force between the overlapping filaments within the Mg^{2+} -induced actin rings might allow them to relax to larger and more variable sizes.

In summary, we report observations of closed loops of F-actin, induced either by 50 mM $MgCl_2$, or by biotin-streptavidin conjugation. For the former case, the interaction energy due to the polyelectrolyte condensation of F-actin is estimated to be of the order of 0.02 kT per actin protomer. For the latter case, actin rings with an average diameter much smaller than the persistence length of F-actin were observed. The findings of various forms of lateral aggregates of actin filaments induced by 50 mM Mg^{2+} ions support the idea that attractive interactions between like-charged linear polymers due to distributions of multivalent counterions, previously verified mainly for the case of DNA, is a general feature for charged biopolymers and can result in a multitude of structure variations.

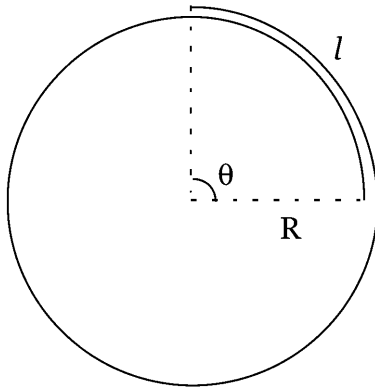
Acknowledgements We acknowledge help from Robijn Bruinsma of UCLA for the derivations shown in the Appendix. We also appreciate assistance from Mr. David Bahk for image analysis. This work was supported by NIH grants AR38910 (PAJ) and HL67286 (JXT), and by NSF-DMR9988389 (JXT) and MRSEC DMR 00-79909 (PAJ).

Appendix

Estimation of adhesion energy based on ring diameter and persistence length

We present here a simple analysis of ring formation, with the goal of relating the adhesion energy to the conformation of the ring, induced either by electrostatic effect, or by specific chemical crosslinkers.

For a ring of diameter R , formed by a single filament of total length L (see Scheme 1):



Scheme 1 Adhesion of two ends of a filament to form a ring

$$L = 2\pi R + l \quad (3)$$

where $l = R\theta$ is the overlap length.

The total Hamiltonian is a sum of bending energy and the adhesion energy between the two ends; hence:

$$\mathfrak{R} = \int ds \kappa(s) \frac{1}{R^2} - vl = \frac{\kappa L}{R^2} + v(2\pi R - L) \quad (4)$$

Note that the integration in the first term covers the entire filament contour, while assuming a constant bending stiffness κ . This assumption is equivalent to integrating over the circumference of the circle only, but assuming the bending stiffness to be 2κ for the segment of overlap.

If one further assumes that the overlap length l is variable via changes in R , and that the ring reaches the extent of overlap that minimizes the Hamiltonian as expressed above, i.e., $\partial\mathfrak{R}/\partial R = 0$, v can be determined by measuring L and R as expressed below:

$$v = \frac{\kappa L}{\pi R^3} = \frac{2kTL_p L}{\pi R^3} \quad (5)$$

where L_p is the persistence length of the filament, which is related to the bending stiffness as $\kappa = 2kTL_p$ (Kas et al. 1993).

If, on the other hand, the overlap between the two ends is not variable, but rather is due to a small number of strong single bonds n , the interaction energy of each bond ϵ is related to the association constant:

$$\epsilon = kT \ln(K_a) \quad (6)$$

The bending energy needed to form a closed loop, if one ignores the overlap region, can be expressed as $2\pi\kappa/R$. By setting this bending energy equal to the binding energy $n\epsilon$ and recalling that $\kappa = 2kTL_p$, one arrives at the expression below:

$$\frac{4\pi kTL_p}{R} = n\epsilon = nkT \ln(K_a) \quad (7)$$

A slight rearrangement of Eq. 1 yields the final expression for the number of bonds as follows:

$$n = \frac{4\pi L_p}{R \ln(K_a)} \quad (8)$$

Equation 8 may be applicable for the case of actin rings formed using streptavidin to crosslink the ends of a biotinylated actin filament. For example, by taking $R = 1.2 \mu\text{m}$ for the average ring radius, $L_p = 17 \mu\text{m}$ for the persistence length of F-actin, and $K_a = 2.5 \times 10^{13} \text{M}^{-1}$ for the association constant of the biotin-streptavidin bond (Green 1990), one obtains $n = 5$ as the average number of bonds required for the ring formation.

References

- Alberts B, Bray D, Lewis J, Raff M, Roberts K, Watson J (1994) Molecular biology of the cell, 3rd edn. Garland, New York
- Baeza I, Gariglio P, Rangel LM, Chavez P, Cervantes L, Arguello C, Wong C, Montanez C (1987) Electron microscopy and biochemical properties of polyamines-compacted DNA. *Biochemistry* 26:6387–6392
- Bloomfield VA (1991) Condensation of DNA by multivalent cations: considerations on mechanism. *Biopolymers* 31:1471–1481
- Carlier MF, Valentin-Ranc C, Combeau C, Fievez S, Pantaloni D (1994) Actin polymerization: regulation by divalent metal ion and nucleotide binding, ATP hydrolysis and binding of myosin. *Adv Exp Med Biol* 358:71–81
- Condeelis J (1993) Life at the leading edge: the formation of cell protrusions. *Annu Rev Cell Biol* 9:411–444
- Dewey TG (1990) A ligand binding model of counterion condensation to finite length polyelectrolytes. *Biopolymers* 29:1793–1799
- Gittes F, Mickey B, Nettleton J, Howard J (1993) Flexural rigidity of microtubules and actin filaments measured from thermal fluctuations in shape. *J Cell Biol* 120:923–934
- Golestanian R, Liverpool TB (2000) Statistical mechanics of semiflexible ribbon polymers. *Phys Rev E* 62:5488–5499
- Green NM (1990) Avidin and streptavidin. *Methods Enzymol* 184:51–67
- Gronbech-Jensen N, Mashl RJ, Bruinsma RF, Gelbart WM (1997) Counterion-induced attraction between rigid polyelectrolytes. *Phys Rev Lett* 78:2477–2480
- Ha B-Y, Liu AJ (1997) Counterion-mediated attraction between two like-charged rods. *Phys Rev Lett* 79:1289–1292
- Isambert H, Venier P, Maggs AC, Fattoum A, Kassab R, Pantaloni D, Carlier M (1995) Flexibility of actin filaments derived from thermal fluctuations. *J Biol Chem* 270:11437–11444
- Kas J, Strey H, Barmann M, Sackmann E (1993) Direct measurement of the wave-vector dependent bending stiffness of freely flickering actin filaments. *Europhys Lett* 21:865–870
- Kas J, Strey H, Tang JX, Finger D, Ezzell R, Sackmann E, Janmey PA (1996) F-actin, a model polymer for semiflexible chains in dilute, semidilute and liquid crystalline solutions. *Biophys J* 70:609–625
- Kawamura M, Maruyama K (1970) Polymorphism of F-actin. I. Three forms of paracrystals. *J Biochem (Tokyo)* 68:885–899
- Lyubartsev AP, Tang JX, Janmey PA, Nordenskiold L (1998) Electrostatically induced polyelectrolyte association of rodlike virus particles. *Phys Rev Lett* 81:5465–5468
- Manning GS (1978) The molecular theory of polyelectrolyte solutions with applications to the electrostatic properties of polynucleotides. *Q Rev Biophys* 11:179–246
- Marquet R, Houssier C (1991) Thermodynamics of cation-induced DNA condensation. *J Biomol Struct Dyn* 9:159–167
- Nguyen TR, Shklovskii BI (2000) Reentrant condensation of DNA induced by multivalent counterions. *J Chem Phys* 112:2562–2568
- Odijk T (1977) Polyelectrolytes near the rod limit. *J Polym Sci Polym Phys Edn* 15:477–483

- Oosawa F (1971) *Polyelectrolytes*. Dekker, New York
- Oosawa F (1993) Physical chemistry of actin: past, present and future. *Biophys Chem* 47:101–111
- Ott A, Magnasco M, Simon A, Libchaber A (1993) Measurement of the persistence length of polymerized actin using fluorescence microscopy. *Phys Rev E* 48:1642–1645
- Ray J, Manning GS (1994) An attractive force between two rodlike polyions mediated by sharing of condensed counterions. *Langmuir* 10:2450–2461
- Rousina I, Bloomfield VA (1996) Macroion attraction due to electrostatic correlation between screening counterions. I. Mobile surface-adsorbed ions and diffuse ion cloud. *J Phys Chem* 100:9977–9989
- Schnurr B, MacIntosh FC, Williams DRM (2000) Dynamical intermediates in the collapse of semiflexible polymers in poor solvents. *Europhys Lett* 51:279–285
- Spudich J, Watt S (1971) The regulation of rabbit skeletal muscle contraction. I. Biochemical studies of the interaction of the tropomyosin-troponin complex with actin and the proteolytic fragments of myosin. *J Biol Chem* 246:4866–4871
- Stossel TP (1993) On the crawling of animal cells. *Science* 260:1086–1094
- Tang JX, Janmey PA (1996) Polyelectrolyte nature of F-actin and mechanism of actin bundle formation. *J Biol Chem* 271:8556–8563
- Tang JX, Wong S, Tran PT, Janmey PA (1996) Counterion induced bundle formation of rodlike polyelectrolytes. *Ber Bunsenges Phys Chem* 100:796–806
- Tang JX, Szymanski P, Janmey PA, Tao T (1997) Electrostatic effects of smooth muscle calponin on actin assembly. *Eur J Biochem* 247:432–440
- Xian W, Tang JX, Janmey PA, Braunlin WH (1999) The polyelectrolyte behavior of actin filaments: a ^{25}Mg NMR study. *Biochemistry* 38:7219–7226
- Yanagida T, Nakase M, Nishiyama K, Oosawa F (1984) Direct observation of motion of single F-actin filaments in the presence of myosin. *Nature* 307:58–60